ACS OMEGA

Open Access

http://pubs.acs.org/journal/acsodf

Article

Rolling Circle Amplification Integrating with Exonuclease-III-Assisted Color Reaction for Sensitive Telomerase Activity Analysis

Xiaoya Liu, Xianxian Zhao, Jie Zhang, Yihan Wang, and Xiaoping Ye*

Cite This: *ACS Omega* 2024, 9, 49081−49087

Read Online

ACCESS | Metrics & More | Article Recommendations | Supporting Information

ABSTRACT: Telomerase activation can lead to the escape from cell senescence and immortalization, playing a crucial role in the growth and proliferation of cancer cells. Therefore, the detection of telomerase activity is essential for cancer diagnosis and treatment. Herein, we develop a novel ultrasensitive and visually detectable platform. By incorporation of exonuclease-III (Exo-III), this platform achieves dual signal amplification of rolling circle amplification products. Additionally, the colorimetric analysis of 3,3′,5,5′-tetramethylbiphenyl (TMB) chromogenic reaction system provides this approach with unique advantages such as simplicity, speediness, and sensitivity. The detection platform exhibits high sensitivity and specificity in actual sample testing, which aligns closely with results obtained using commercial kits. Moreover, it offers ease-of-use through visual determination by the naked eyes. This finding indicates that our proposed sensing method performs satisfactorily in detecting telomerase in real biological samples. Henceforth, we believe that this sensing platform holds great potential for clinical diagnosis and anticancer drug development.

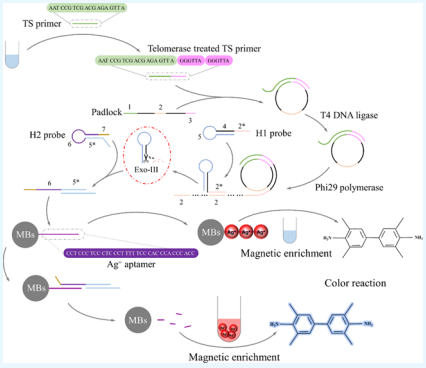

1. INTRODUCTION

Telomerase, a ribonucleoprotein complex, is responsible for synthesizing telomere DNA repeats at the chromosome ends and counteracting DNA loss during replication.[1−3] By utilizing the RNA sequence carried by telomerase as the template, telomere DNA extends to generate numerous repetitive sequences, enabling cells to proliferate rapidly and indefinitely. Studies have identified limitless replicative potential as one of cancer's hallmarks, which is associated with the activation of telomerase maintenance mechanisms.[4−6] The presence of telomerase was detected in nearly all human tumor cells. Consequently, targeting telomerase has emerged as a promising approach for cancer diagnosis, prognosis, and treatment.[7−9] Therefore, precise and efficient detection methods for telomerase hold significant value in cancer research and therapy.

The telomeric repeat amplification protocol (TRAP), based on the polymerase chain reaction (PCR), is widely employed for the detection of telomerase.[10−12] Incorporating PCR amplification significantly enhances the sensitivity of telomerase detection. Enzyme-linked immunosorbent assay (ELISA) utilizes antidigoxin antibody conjugated with peroxidase to detect immobilized amplification products. This method is characterized by its simplicity, sensitivity, specificity, and ease of quantitative analysis. However, the TRAP method suffers from certain drawbacks, including susceptibility to contamination, high cost, complex operation, and time-consuming procedures, as well as poor repeatability. ELISA is prone to false positives due to numerous interfering factors that limit its clinical applicability.[13−15] In light of advancing research on telomerase, novel detection technologies such as fluorescence-based assays, electrochemical methods, and chemiluminescence have been proposed.[16−18] However, these techniques require further improvement in terms of sensitivity since they lack signal amplification processing. Moreover, once telomerase is identified during the sensing process, concerns arise regarding insufficient specificity. Furthermore, the complexity associated with designing these methods also restricts their wider application in telomerase detection.[19,20] Therefore, it is imperative to develop a portable platform capable of accurately and sensitively analyzing telomerase detection methods.

Isothermal amplification technology is a novel amplification technique that follows PCR.[21−23] This method operates at a constant temperature, eliminating the need for complex temperature cycling, and offers advantages such as high efficiency, rapidity, and excellent specificity. Incorporating isothermal nucleic acid amplification technology holds great potential to significantly enhance the sensitivity of telomerase detection. Among these techniques, rolling circle amplification (RCA) stands out as one of the prominent isothermal methods currently available due to its simplicity in operation, high specificity, and broad applicability.[24−26] For instance, Deng et

Received: April 22, 2024
Revised: October 7, 2024
Accepted: November 25, 2024
Published: December 4, 2024

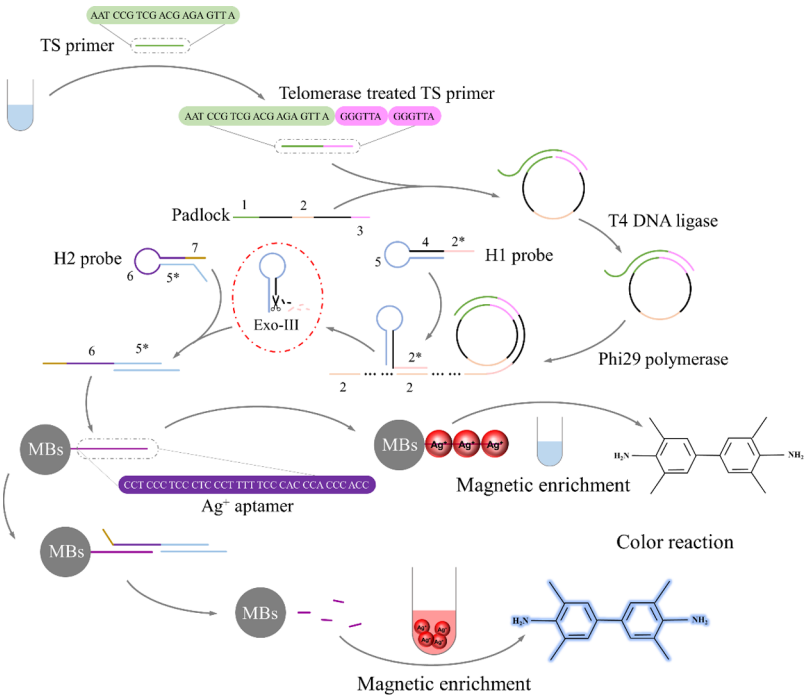

Figure 1. Working mechanism of the sensing system for telomerase detection.

al. successfully established a robust and highly sensitive detection platform for EGFR 19 utilizing RCA which exhibited exceptional performance in detecting targets within complex serum samples as well as cell genomes.[27] However, further improvement is required in the sensitivity of RCA. Exonuclease-III (Exo-III) is an enzyme with multifunctional capabilities.[28,29] It efficiently and stably cleaves DNA double-stranded molecules with blunt ends or recessed 3′-ends from the 3′→5′ direction, releasing single nucleotides without the need for specific recognition sites. Exo-III possesses various signal output and amplification methods, enabling the rapid and accurate detection of target substances. Integrating Exo-III-based signal cycling strategy is anticipated to enhance the signal amplification efficiency of RCA-based detection technology.[30] Min et al. developed a sensitive and convenient method for telomerase detection using a probe (TPE-Py-DNA) as a fluorescence reporter and Exo-III as a signal amplifier.[31] However, this fluorescence-based telomerase detection requires labeling fluorescent dyes, which carry the risk of fluorescence contamination and necessitates specialized instruments to detect changes in fluorescence, making it challenging to visually display the results with the naked eyes. Therefore, constructing a sensitive, accurate, and visually interpretable telomerase detection technology holds significant importance.

Herein, we depict a novel sensitive, accurate, and visible telomerase detection method by integrating the Exo-III-assisted RCA-based signal amplification strategy with the Ag^+ aptamer-based color reaction. The extended telomerase primer was used to characterize the activity of the telomerase, and the extended telomerase primer product could initiate the RCA process and the Exo-III-assisted signal cycle. By integrating with the Ag^+-aptamer@ magnetic bead (MB)-based color reaction, the detection result could be directly read by the naked eyes. This approach offers robust technical support for telomerase detection and holds promising potential for guiding early tumor screening, diagnosis, and treatment.

2. EXPERIMENTAL SECTION

2.1. Materials and Reagents. All of the essential nucleic acid oligonucleotides utilized in this research were procured from Sangon Biotech Co., Ltd. (Shanghai, China), with detailed sequences provided in Table S1. The T4 DNA ligase, Phi29 DNA polymerase, dNTPs, and Exo-III enzyme employed for signal amplification were obtained from New England Biolabs (Shanghai, China). DEPC water was acquired from Sigma−Aldrich. 3,3′,5,5′-Tetramethylbiphenyl (TMB) was acquired from Sigma-Aldrich (Shanghai, China). All relevant reagents were of analytical grade.

2.2. Cell Culture and Telomerase Extraction. HeLa cells were cultured in a biochemical incubator. Cell lysate was added to complete cell lysis, and the extract containing telomerase was frozen at −80 °C for use.

2.3. Extended Reaction. 2 μL of telomerase, 2 μL of TS primer, 2 μL of dNTPs, and 4 μL of buffer were mixed and incubated at 37 °C for 1 h followed by 90 °C for 10 min and then cooled to room temperature. The extended product, synthesized padlock, was rehydrated into a 10 μM concentration and ligated using T4 DNA ligase to form the desired structure in a metal dry bath (Thermo Scientific, USA) at 37 °C for 1 h. The ligation experiments were performed in a 20 μL mixture consisting of 10 μL of extended product, 2 μL of padlock (10 μM), 1 μL of T4 DNA ligase (400 U/μL), 5 μL of ligase buffer (10×), and 2 μL of DEPC water.

2.4. RCA Reaction. The RCA reaction was performed in a 40 μL mixture comprising 20 μL of ligation products, 4 μL of reaction buffer (10×), 1 μL of BSA (10 mg/mL), 5 μL of dNTP (2.5 mM), 1 μL of Phi29 DNA polymerase (10 U/μL), and 9 μL of DEPC water. The reaction mixture was incubated at 37 °C for 2 h and subsequently denatured at 65 °C for 10 min, followed by gradually cooling to room temperature.

https://doi.org/10.1021/acsomega.4c03839
ACS Omega 2024, 9, 49081−49087

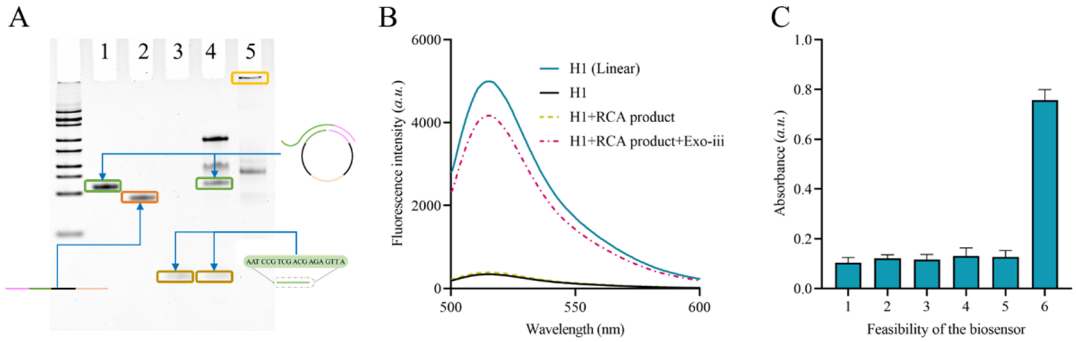

Figure 2. Feasibility analysis of the proposed method. (A) PAGE result of the telomerase-based RCA process. Line 1: primer product+ padlock; line 2: padlock; line 3: primer; line 4: primer product+ padlock+ phi29 polymerase+ T4 DNA ligases; and line 5: primer product+ padlock+ phi29 polymerase+ T4 DNA ligase+ telomerase. (B) Fluorescence spectrum of the FAM labeled H1 probe when incubated with Exo-III. (C) Absorbance of the approach for telomerase activity analysis when essential experimental components existed or not. Column 1: tolemerase (−); column 2: T4 DNA ligase; column 3: phi29 polymerase (−); column 4: H1 probe (−); column 5: Exo-III (−); and column 6: with all.

2.5. Color Reaction. 2 μL of Exo-III (0.5 unit/μL) and 2 μL of hairpin recognition chain were added to the RCA product and incubated at 37 °C for 30 min. Subsequently, 2 μL H2 probe (1 nM) and 2 μL Exo-III (0.5 unit/μL) were added to the above solution and further incubated at room temperature for 30 min. Two μL aptamer@MB. Ag^+ (5 μM) was added to the obtained solution and incubated with rapid oscillation for 3 min, subsequently separated by a hopper magnet, and washed by buffer solution, followed by 2 μL TMB (0.4 nM). Upon the completion of the reaction, the color change of the solution was visually observed, and the fluorescence intensity of the system was recorded by Hitachi fluorescence spectrometer F-6700 (Beijing, China). The sensitivity of the method was evaluated by detecting different concentrations of telomerase. Correction between the obtained fluorescence intensity and concentration of telomerase was calculated by GraphPad 8.0.

3. RESULTS AND DISCUSSION

3.1. Principle of the Detection Platform. The principle of the proposed telomerase detection method is illustrated in Figure 1. When telomerase is present in the sensing system, the telomerase primers can be extended to produce repetitive sequences that can bind to padlock probes, creating a circular DNA molecule with a gap. These gaps at the ends are linked together to create a closed circular template for the replication of nucleic acid chains with the assistance of T4 DNA ligase. With the closed circular DNA as a template, phi29 DNA polymerase is used as an enzyme catalyst that allows for the replication and elongation of the nucleic acid chain, resulting in the production of RCA products that contain repetitive sequences "2". The H1 probe selectively recognizes the nucleotide "2" and creates double-stranded structures with a blunt 5′ terminal when hybridized with "2" sections.

The Exo-III efficiently and stably cleaves DNA double-stranded molecules with blunt 5′ ends from the 3′→5′ direction, releasing single nucleotides without the need for specific recognition sites. Therefore, the Exo-III could recognize the blunt 5′ terminal and cleave the "2*" and "4" sections in the H1 probe, releasing "5" sequence to mediate signal reaction. The "5" sequences unfold the H2 probe via binding with the "5*" section, exposing the "6" and "7" sections. The inclusion of an H2 probe enhances the ability to connect with cleavage products and causes the unfolding of hairpin structures, resulting in the production of double-stranded DNAs with sticky ends. The aptamer sequences loading on the surface of MBs, which is referred to as aptamer@MB, bind with the "6" section in the H2 probe to form a sticky end. When telomerase is present, Exo-III recognizes the sticky end and cleaves Ag^+ aptamer. As a result, the Ag^+ ions remain in the sensing system when the aptamer@MB was removed to induce the TMB-based color reaction. In detail, the silver ions were chelated by aptamer sequences via the interaction between Ag^+ and N3 of cytosine (C), forming a strong and stable "C−Ag^+-C" hairpin structure. The digestion of the aptamer by Exo-III released Ag^+ to oxidize TMB for coloring. The solution that contained oxidized TMB (TMBox) had a blue color. On the other hand, when the target is not present, the Ag^+ aptamer stays undamaged and successfully catches Ag^+ ions. These ions are then removed by washing them away with the Ag^+-aptamer@MB complex. As a result, there are no Ag^+ ions present in the sensor system, which prevents the commencement of any color reaction for visual detection. Absorbance measurements can be used to accurately quantify telomerase levels.

3.2. Feasibility of the Method. PAGE result demonstrated that the telomerase-treated TS primer could mediate the RCA process, thus producing a long ssDNA product in lane 5 (Figure 2A). The band in line 1 is the complex of primer product and the padlock, which moves slower than the primer (line 3) or padlock alone (line 2). When all essential components exist in the sensing system, the RCA product is blocked in the loading well (line 5). As control, no band is blocked in the loading well in the absence of telomerase. The cleavage of the activated Exo-III enzyme toward the H1 probe was initially verified (Figure S1). Figure 2B demonstrates the successful assembly of the H1 probe, where the fluorophore-labeled "5" section (FAM-"5") is connected to the quencher-labeled "3" section (BHQ1-"3"). The reduction in fluorescence signal reflects the nearness of the fluorophore to the quencher and the successful formation of the "stem" segment in the H1 probe. Furthermore, the quenched signal remains low when the assembled H1 probe is incubated with the rolling circle amplification product. The result demonstrates the efficient cleavage of the "2*" and "4" regions by Exo-III. The efficient and firm fixation of the silver ion aptamer on the MBs surface determines the color reaction because magnetic enrichment and separation are necessary. Therefore, we verified the assembly of Ag^+@MBs by labeling the 5′-end of Ag^+ aptamer with a FAM moiety. The results showed that when the Ag^+

https://doi.org/10.1021/acsomega.4c03839
ACS Omega 2024, 9, 49081−49087

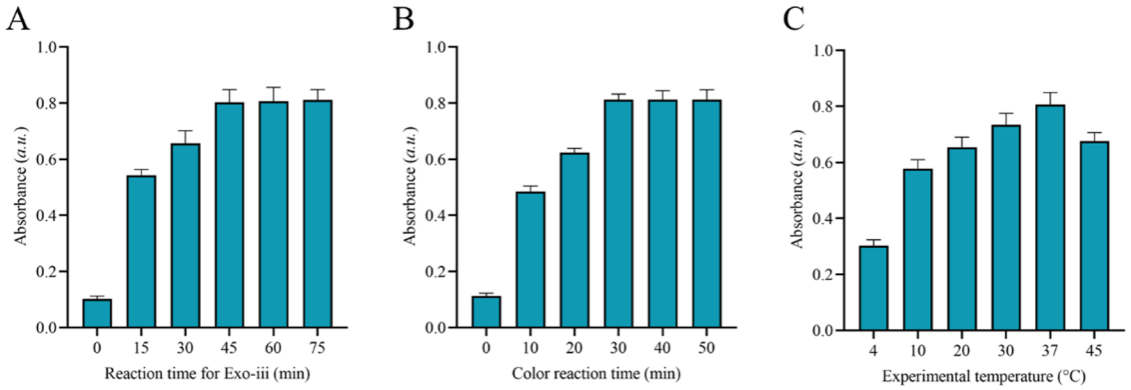

Figure 3. Optimization of experimental parameters. Absorbance of the approach when detecting telomerase activity with different reaction times for Exo-III (A), different color reaction times (B), and experimental temperatures (C).

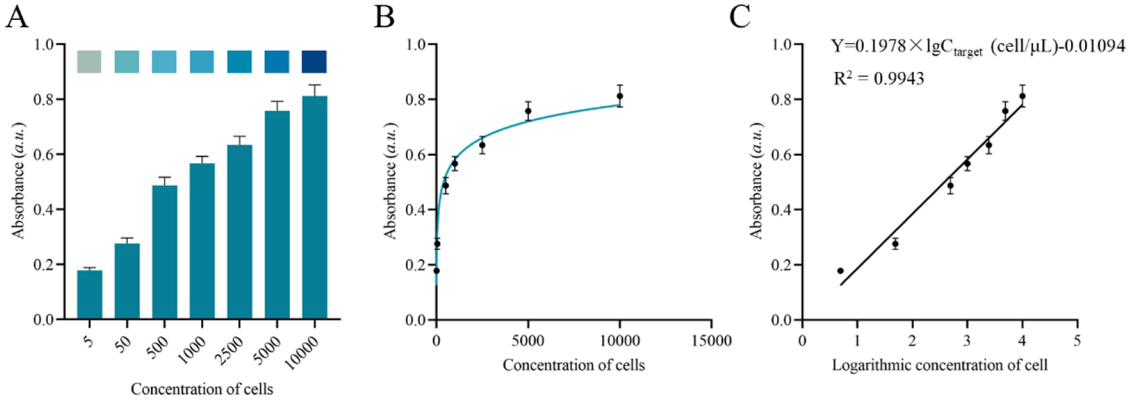

Figure 4. Analytical performance of the approach. (A) Absorbance of the approach when detecting telomerase activity from different concentrations of cells. (B) Correlation between the absorbance of the method and the logarithmic concentration of cells.

aptamer was fixed on the surface of MBs, the FAM fluorescence signal in the supernatant was significantly reduced after magnetic enrichment and separation (Figure S2).

The practicality of the method was confirmed by using a color reaction. Significant color changes from colorless to blue were seen when the target telomerase, necessary enzymes, H1 probe, and Exo-III were all present. No significant color changes were seen when any of the experimental components were absent, indicating that these components play a crucial role in the method's viability (Figure 2C).

3.3. Optimization of Reaction Conditions for Improving Analytical Performance. The best parameters for this approach were discovered by comparing the absorbances under different reaction circumstances. The reaction parameters, including duration and temperature, were optimized by detecting telomerases. For an improved detection efficiency, the reaction times of Exo-III were first optimized. Figure 3A clearly illustrates an increasing tendency in absorbance as the response time of Exo-III grows from 0 to 45 min, eventually reaching an equilibrium. The results indicate that the activated Exo-III enzyme may fully cleave the H1 probe within 45 min, which was determined the optimized reaction duration. Figure 3B illustrates a gradual increase in absorbance as the duration of the color response grows from 0 to 30 min, after which it stabilizes. Therefore, the optimal response time for the color reaction is 30 min. The subsequent experiment aimed to identify the optimal reaction temperatures for generating the highest level of signal amplification efficiency. Figure 3C shows a gradual increase in absorbance as the reaction temperature increases from 4 to 37 °C. However, it thereafter experiences a significant decline, indicating that temperatures over 37 °C have an adverse impact on the transcleavage activity of Exo-III. Therefore, the temperature at which the sensor system reacts is 37 °C. Furthermore, the H1 concentration, H2 concentration, and Ag^+ were optimized. The results in Figures S3−S5 showed that the optimized concentrations for H1 probe, H2 probe, and Ag^+ were 100, 100 nM, and 5 mM, respectively.

3.4. Ultrahigh Sensitivity of this Method for Telomerase Detection. The sensitivity of the biosensor is crucial due to the relatively low amount of telomerase, especially in the early stages of the disease. Thus, we assessed the sensitivity of the colorimetric technique using rolling circle amplification-triggered exonuclease-III under the optimized experimental parameters. The telomerase, which is isolated from HeLa cells, is used as the detection sample. As the number of HeLa cells increased, it was observed that an increasing number of TS primer and padlock strands participated in subsequent RCA, resulting in color alterations (Figure 4A, inset is the color result). The absorbance values increase gradually as the concentration of extracted telomerase from cells increases, as shown in Figure 4B. The relationship between absorbance values and logarithmic values of cell concentrations ranging from 5 to 10,000 is linear, as depicted in Figure 4C. The equation that represents this relationship is $Y = 0.1978 \times \lg C_{target}\ (\text{cell}/\mu\text{L}) - 0.01094$, and the correlation coefficient (R^2) is 0.9943. At a signal-to-noise ratio of 3, the estimated limit of detection (LOD) is 3.12 cell/μL, which is

https://doi.org/10.1021/acsomega.4c03839
ACS Omega 2024, 9, 49081−49087

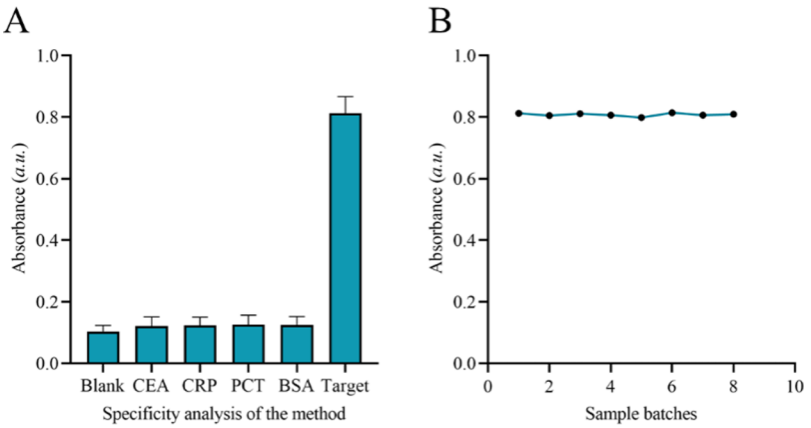

Figure 5. Specificity of the method. (A) Absorbance of the method for telomerase and interfering molecule detection. (B) Absorbance of the approach when detecting telomerase from 8 samples.

superior to or comparable to the LODs of numerous colorimetric techniques (Table S2).[11,12,16,19]

3.5. Specificity and Reproducibility of this Method. To evaluate the specificity of the proposed Exo-III-assisted colorimetric approach, we conducted an experiment. Four interfering protein molecules, namely, CEA, CRP, PCT, and BSA, were introduced into the system. The results in Figure 5A showed that the color changes of the interfering protein molecules were all negligible compared to the blank control. Nevertheless, a notable rise in absorbance values was solely found for telomerase. The aforementioned results provided evidence of the suggested approach's remarkable specificity in detecting telomerase. To further validate the replicability of the devised procedure (Figure 5B), telomerase levels were evaluated in eight sample duplicates using the proposed strategy. Therefore, the suggested technique demonstrated satisfactory repeatability, as evidenced by the achieved relative standard deviation (RSD) of 3.442%.

3.6. Clinical Sample Detection and Methodology Comparison. As part of the recovery investigation, we conducted three separate analyses of samples containing telomerase extracted from cells in varying quantities to verify the stability of the approach. Table 1 displays the recoveries,

Table 1. Recovery Test of the Method

samples	added (cell/μL)	recovered (cell/μL)	recovery rate (%)
1	100	99.5	99.5
2	1000	1026	102.6
3	5000	4921	98.43

which varied from 98.43 to 102.6%, with RSDs ranging from 3.74 to 4.42%, indicating the high anti-interference capability. In addition, the proposed method was compared to the quantitative outcome achieved using commercially available telomerase detection kits. Figure 6 depicts the numerical result. The outcomes of our approach showed a strong correlation with the telomerase amounts determined with the commercially available kit. The results indicate that the test demonstrated satisfactory accuracy in measuring telomerase levels in a genuine biological sample. Therefore, it shows potential as a method for detecting telomerase derived from cancer cells.

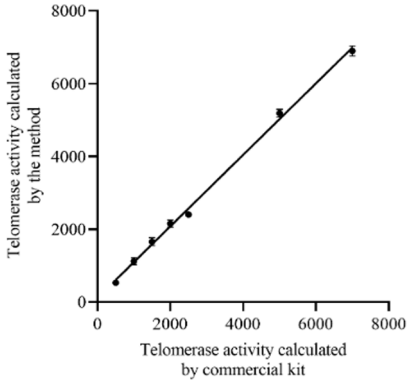

Figure 6. Correlation between the calculated telomerase activity by the method and the commercial kit.

4. CONCLUSIONS

To summarize, we have created a highly sensitive and effective colorimetric method for telomerase detection by combining the TS primer extension-based RCA, Exo-III-assisted signal recycling, and color reaction. This proposed strategy offers several notable benefits: (i) the utilization of Exo-III enzyme and RCA-assisted dual signal amplification provides the biosensor with exceptional sensitivity; (ii) the colorimetric detection, coupled with naked eye visualization, offers convenient point-of-care usage; and (iii) the inclusion of aptamer@MB complex enhances the biosensor's ability to resist interference. Furthermore, it showcases an exceptional analytical prowess by effectively identifying samples. The advantages outlined above indicate considerable potential for using telomerase detection-based liquid biopsy to enable fast and precise cancer diagnosis at the point of care.

■ ASSOCIATED CONTENT

Supporting Information

The Supporting Information is available free of charge at https://pubs.acs.org/doi/10.1021/acsomega.4c03839.

Illustration of the fluorescence assay to test the Exo-III-assisted cleavage of H1 probe; fluorescence intensity of the FAM labeled Ag^+ aptamer before and after assembled with MBs; optimization of the H1 probe concentration; absorbance of the method when detecting target with different concentrations of H1 probe (nM); optimization of the H2 probe concen-

https://doi.org/10.1021/acsomega.4c03839
ACS Omega 2024, 9, 49081−49087

tration; absorbance of the method when detecting target with different concentrations of H2 probe (nM); optimization of the Ag^+ concentration; absorbance of the method when detecting target with different concentrations of Ag^+ (mM); sequences of the oligonucleotides used in present study; and brief comparison of the approach with former ones (PDF)

AUTHOR INFORMATION

Corresponding Author

Xiaoping Ye − *Department of Ultrasound, The First Affiliated Hospital of Chongqing Medical University, Chongqing 400016, China;* orcid.org/0000-0002-2752-060X; Email: yxplh051224@163.com

Authors

Xiaoya Liu − *Department of Oncology, The First Affiliated Hospital of Chongqing Medical University, Chongqing 400016, China*

Xianxian Zhao − *Central Laboratory, Chongqing University FuLing Hospital, Chongqing 408099, China;* orcid.org/0000-0002-8118-204X

Jie Zhang − *Department of Oncology, The First Affiliated Hospital of Chongqing Medical University, Chongqing 400016, China*

Yihan Wang − *Department of Oncology, The First Affiliated Hospital of Chongqing Medical University, Chongqing 400016, China*

Complete contact information is available at: https://pubs.acs.org/10.1021/acsomega.4c03839

Author Contributions

X.Y.: visualization, writing—review, editing, supervision, and funding acquisition; X.L.: methodology, formal analysis, investigation, data curation, and writing—original draft; and X.Z., J.Z., and Y.W.: formal analysis and investigation.

Notes

The authors declare no competing financial interest.

ACKNOWLEDGMENTS

The authors thank financial support from National Natural Science Foundation of China (no. 82202645).

REFERENCES

(1) Kumar, N.; Sethi, G. Telomerase and hallmarks of cancer: An intricate interplay governing cancer cell evolution. *Cancer Lett.* **2023**, *578*, No. 216459.

(2) Saretzki, G. Role of Telomeres and Telomerase in Cancer and Aging. *Int. J. Mol. Sci.* **2023**, *24* (12), 9932.

(3) Liu, M.; Zhang, Y.; Jian, Y.; Gu, L.; Zhang, D.; Zhou, H.; Wang, Y.; Xu, Z. X. The regulations of telomerase reverse transcriptase (TERT) in cancer. *Cell Death Dis.* **2024**, *15* (1), 90.

(4) Guo, Y.; Li, S.; Tong, Z.; Tang, J.; Zhang, R.; Lv, Z.; Song, N.; Yang, D.; Yao, C. Telomerase-Mediated Self-Assembly of DNA Network in Cancer Cells Enabling Mitochondrial Interference. *J. Am. Chem. Soc.* **2023**, *145* (43), 23859−23873.

(5) Revy, P.; Kannengiesser, C.; Bertuch, A. A. Genetics of human telomere biology disorders. *Nat. Rev. Genet* **2023**, *24* (2), 86−108.

(6) Perez-Lopez, F. R.; Ulloque-Badaracco, J. R.; Lopez-Baena, M. T.; Yuan, J.; Alarcon-Braga, E. A.; Benites-Zapata, V. A. Endometrial telomerase activity in women with either endometrial cancer or hyperplasia: A systematic review and meta-analysis. *Maturitas* **2023**, *174*, 57−66.

(7) Vishwakarma, K.; Dey, R.; Bhatt, H. Telomerase: A prominent oncological target for development of chemotherapeutic agents. *Eur. J. Med. Chem.* **2023**, *249*, No. 115121.

(8) D'Alessandris, Q. G.; Battistelli, M.; Pennisi, G.; Offi, M.; Martini, M.; Cenci, T.; Falchetti, M. L.; Lauretti, L.; Olivi, A.; Pallini, R. Telomerase inhibition in malignant gliomas: a systematic review. *Expert Rev. Mol. Med.* **2023**, *25*, No. e10.

(9) Bruedigam, C.; Porter, A. H.; Song, A.; In, Vroeg; de Wei, G.; Stoll, T.; Straube, J.; Cooper, L.; Cheng, G.; Kahl, V. F. S.; Sobinoff, A. P. Imetelstat-mediated alterations in fatty acid metabolism to induce ferroptosis as a therapeutic strategy for acute myeloid leukemia. *Nat. Cancer* **2024**, *5* (1), 47−65.

(10) Fajkus, J. Detection of telomerase activity by the TRAP assay and its variants and alternatives. *Clin. Chim. Acta* **2006**, *371* (1−2), 25−31.

(11) Afshari, N.; Al-Gazally, M. E.; Rasulova, I.; Jalil, A. T.; Matinfar, S.; Momeninejad, M. Sensitive bioanalytical methods for telomerase activity detection: a cancer biomarker. *Anal Methods* **2022**, *14* (42), 4174−4184.

(12) Wang, J.; Liu, X.; Xue, W.; Wei, Y.; Xu, Z. Highly sensitive monitoring of telomerase activity in living cells based on rapidly triggered cascade amplification reaction. *Biosens Bioelectron* **2022**, *216*, No. 114645.

(13) Tsoukalas, D.; Buga, A. M.; Docea, A. O.; Sarandi, E.; Mitrut, R.; Renieri, E.; Spandidos, D. A.; Rogoveanu, I.; Cercelaru, L.; Niculescu, M. Reversal of brain aging by targeting telomerase: A nutraceutical approach. *Int. J. Mol. Med.* **2021**, *48* (5), 199.

(14) Zarei, R.; Moghadam, D.; Sarabi, M. M.; Naghibalhossaini, F. The effect of benzo[alpha]pyrene on DNA methylation and telomerase activity in human normal and cancer cells. *Toxicol In Vitro* **2022**, *80*, No. 105331.

(15) Li, L.; Zhang, H.; Chen, B.; Xia, B.; Zhu, R.; Liu, Y.; Dai, X.; Ye, Z.; Zhao, D.; Mo, F.; et al. BaZiBuShen alleviates cognitive deficits and regulates Sirt6/NRF2/HO-1 and Sirt6/P53-PGC-1alpha-TERT signaling pathways in aging mice. *J. Ethnopharmacol* **2022**, *282*, No. 114653.

(16) Ma, D.; Bai, H.; Li, J.; Li, Y.; Song, L.; Zheng, J.; Miao, C. A ratiometric fluorescent nanoprobe for signal amplification monitoring of intracellular telomerase activity. *Anal Bioanal Chem.* **2022**, *414* (5), 1891−1898.

(17) Meng, F.; Chai, H.; Ma, X.; Tang, Y.; Miao, P. FRET investigation toward DNA tetrahedron-based ratiometric analysis of intracellular telomerase activity. *J. Mater. Chem. B* **2019**, *7* (11), 1926−1932.

(18) Gao, Z.; Xu, M.; Hou, L.; Chen, G.; Tang, D. Magnetic bead-based reverse colorimetric immunoassay strategy for sensing biomolecules. *Anal. Chem.* **2013**, *85* (14), 6945−6952.

(19) Gu, Y.; Li, Y.; Ge, S.; Lu, W.; Mao, Y.; Chen, M.; Qian, Y. A SERS Biosensor Based on Functionalized Au-SiNCA Integrated with a Dual Signal Amplification Strategy for Sensitive Detection of Telomerase Activity During EMT in Laryngeal Carcinoma. *Int. J. Nanomedicine* **2023**, *18*, 2553−2565.

(20) Cheng, L.; Zhang, S.; Wang, M.; Lopez-Beltran, A. Biological and clinical perspectives of TERT promoter mutation detection on bladder cancer diagnosis and management. *Hum Pathol* **2023**, *133*, 56−75.

(21) Zhang, X.; Lou, X.; Xia, F. Advances in the detection of telomerase activity using isothermal amplification. *Theranostics* **2017**, *7* (7), 1847−1862.

(22) Yu, P.; Yang, T.; Zhang, D.; Xu, L.; Cheng, X.; Ding, S.; Cheng, W. An all-in-one telomerase assay based on CRISPR-Cas12a trans-cleavage while telomere synthesis. *Anal. Chim. Acta* **2021**, *1159*, No. 338404.

(23) Boonbanjong, P.; Treerattrakoon, K.; Waiwinya, W.; Pitikultham, P.; Japrung, D. Isothermal Amplification Technology for Disease Diagnosis. *Biosensors (Basel)* **2022**, *12* (9), 677.

(24) Xu, L.; Duan, J.; Chen, J.; Ding, S.; Cheng, W. Recent advances in rolling circle amplification-based biosensing strategies-A review. *Anal. Chim. Acta* **2021**, *1148*, 238187.

(25) Yue, S.; Li, Y.; Qiao, Z.; Song, W.; Bi, S. Rolling Circle Replication for Biosensing, Bioimaging, and Biomedicine. *Trends Biotechnol* **2021**, *39* (11), 1160−1172.
(26) Bialy, R. M.; Mainguy, A.; Li, Y.; Brennan, J. D. Functional nucleic acid biosensors utilizing rolling circle amplification. *Chem. Soc. Rev.* **2022**, *51* (21), 9009−9067.
(27) Deng, L.; Zhou, S.; Dong, J.; Liu, Y.; Huang, Z.; Sun, H.; Jin, L.; Huo, D.; Hou, C. CRISPR/Cas12a and primer-assisted rolling circle amplification integrated ultra-sensitive dual-signal sensing platform for EGFR 19 detection. *Anal. Chim. Acta* **2023**, *1279*, No. 341755.
(28) Zhang, M.; Yang, Y.; Xin, L.; Zhang, H.; Wu, L.; Zhu, J.; Zhu, J.; Liu, S.; Wang, Z.; Chen, Q. CSDR Coupling with Exo III for Ultrasensitive Electrochemistry Determination of miR-145. *Molecules* **2023**, *28* (5), 2208.
(29) Ji, Y.; Guo, J.; Ye, B.; Peng, G.; Zhang, C.; Zou, L. An ultrasensitive carcinoembryonic antigen electrochemical aptasensor based on 3D DNA nanoprobe and Exo III. *Biosens Bioelectron* **2022**, *196*, No. 113741.
(30) Zhao, X.; Yuan, Y.; Liu, X.; Mao, F.; Xu, G.; Liu, Q. A Versatile Platform for Sensitive and Label-Free Identification of Biomarkers through an Exo-III-Assisted Cascade Signal Amplification Strategy. *Anal. Chem.* **2022**, *94* (4), 2298−2304.
(31) Min, X.; Xia, L.; Zhuang, Y.; Wang, X.; Du, J.; Zhang, X.; Lou, X.; Xia, F. An AIEgens and exonuclease III aided quadratic amplification assay for detecting and cellular imaging of telomerase activity. *Sci. Bull. (Beijing)* **2017**, *62* (14), 997−1003.

https://doi.org/10.1021/acsomega.4c03839
ACS Omega 2024, 9, 49081−49087